Human Cell (2019) 32:22–30
https://doi.org/10.1007/s13577-018-0220-3

RESEARCH ARTICLE

# Icariin ameliorates angiotensin II-induced cerebrovascular remodeling by inhibiting Nox2-containing NADPH oxidase activation

**Huanhuan Dong[1,2] · Shuping Ming[1,2] · Jie Fang[1,2] · Yun Li[1,3] · Ling Liu[1,3]**

Received: 19 August 2018 / Accepted: 3 October 2018 / Published online: 1 November 2018


## Abstract

Cerebrovascular smooth muscle cells (SMCs) hyperplasia is an important contributor to cerebrovascular remodeling during hypertension. The aim of present study was to investigate the effects of Icariin on cerebrovascular SMCs proliferation and remodeling and the underlying mechanisms. The results revealed that Icariin administration attenuated the enhanced basilar artery constriction in angiotensin II (AngII)-induced hypertension rat model, as well as the inhibition of basilar artery diameter reduction in response to AngII and phenylephrine. In addition, histological analyses showed that Icariin also significantly ameliorated basilar artery remodeling in AngII hypertensive rats. In human brain vascular SMCs (HBVSMCs), AngII-induced cell proliferation, migration and invasion were markedly inhibited by Icariin treatment. Moreover, Icariin treatment largely limited AngII-induced the increase of reactive oxygen species (ROS) production in HBVSMCs, which was closely associated with cell proliferation. Analysis of the mechanisms showed that Icariin decreased ROS production via inhibiting NADPH oxidase activity but not mitochondria-derived ROS production. Further, Icariin promoted Nox2 degradation and consequently reduced its protein expression. In conclusion, these findings demonstrate that Icariin attenuates cerebrovascular SMCs hyperplasia and subsequent remodeling through inhibiting Nox2-containing NADPH oxidase activation, suggesting Icariin may be a potential therapeutic agent to prevent the onset and progression of stroke.

**Keywords** Cerebrovascular remodeling · Proliferation · Reactive oxygen specie · NADPH · Nox2 · Icariin

## Introduction

Cardiovascular diseases threaten health with increasing morbidity and mortality worldwide [1]. Stroke is a severe cardiovascular disease that constitutes the major cause of death [2]. Multiple lines of evidences have indicated that cerebrovascular remodeling due to cerebrovascular smooth muscle cells (SMCs) hyperplasia is responsible for stroke [2–4]. Excessive proliferation and migration of SMCs increases the ratio of wall to lumen diameter in basilar artery, resulting in blood pressure elevation and end-organ damage [4, 5]. Angiotensin II (AngII) plays an important role in the development of vascular remodeling, stroke and hypertension [6, 7]. It activates diverse signaling responses, such as AngII type 1 receptor activation, mitochondrial dysfunction and reactive oxygen species (ROS) production [6, 8, 9]. Among them, ROS is known to be a critical factor for vascular SMCs proliferation and has been implicated in remodeling [10, 11]. Inhibition of excessive ROS production is emerging as a promising strategy for the treatment of cerebrovascular remodeling and stroke [12].

Icariin is a prenylated flavonol glycoside derived from *Epimedium* spp., a traditional Chinese medicine widely used for osteoporosis treatment [13]. Recent studies have exhibited the cardiovascular protective activity of Icariin [14–16]. It has been previously demonstrated that Icariin effectively alleviated myocardial ischemia–reperfusion

**Electronic supplementary material** The online version of this article (https://doi.org/10.1007/s13577-018-0220-3) contains supplementary material, which is available to authorized users.

✉ Ling Liu
liuling_hbtcm@163.com

[1] Department of Encephalopathy, Hubei Provincial Traditional Chinese Medicine Hospital, Wuhan, People's Republic of China

[2] Department of Encephalopathy, Hubei Institute of Traditional Chinese Medicine, Wuhan, People's Republic of China

[3] Department of Encephalopathy, The Affiliated Hospital of Hubei University of Traditional Chinese Medicine, No. 4 Huayuan Hill, Wuchang District, Wuhan 430061, Hubei, People's Republic of China

injury in diabetic rats [17]. Furthermore, several studies have evidenced that Icariin could attenuate cardiomyocyte apoptosis and cardiac remodeling [15, 16, 18]. More importantly, Icariin significantly inhibited ox-LDL-induced the proliferation of vascular SMCs [19]. However, the effects of Icariin on cerebrovascular SMCs proliferation and remodeling are still unknown. In the present study, we demonstrate that Icariin prevents AngII-induced human brain SMC (HBVSMCs) proliferation and cerebrovascular remodeling in hypertensive rats, suggesting that Icariin may be a novel application on stroke treatment.

## Methods and materials

### Materials and reagent

Icariin was obtained from Yunnan Plant Pharmaceutical Factory (purity ≥ 98%; Yunan, China) and dissolved in saline with ultra-sonication. Smooth muscle cell medium, penicillin, streptomycin and fetal bovine serum (FBS) were purchased from ScienceCell Research Laboratories (CA, USA). Angiotensin II (AngII), phenylephrine (Phe), *N*-acetyl-L-cysteine (NAC), 2′,7′-dichlorofluorescin diacetate ($H_2$DCF-DA), dihydroethidium (DHE), MitoSOX red reagent, lucigenin, NADPH, cycloheximide (CHX), and bromodeoxyuridine (BrdU) were purchased from Sigma Chemical Co. (MO, USA). Antibodies against Rac1, p22phox, p47phox, α-SMA and GAPDH were from Santa Cruz Biotechnology (CA, USA). P40phox, p67phox and Nox2 were obtained from Abcam (MA, USA). Rabbit anti-mouse-cy3 secondary antibody, horseradish peroxide-conjugated secondary antibodies, and radioimmuno precipitation assay (RIPA) buffer were from Beyotime (Jiangsu, China).

### AngII-induced hypertension model

6-week-old (180–200 g) Sprague–Dawley rats were purchased from the Animal Center of Guangdong Province (China). All animals were housed with free access to food and tap water under a constant temperature (22–25 °C) and humidity (55 ± 5%) at a 12-h light/12-h dark cycle. The experimental protocol was approved by the Animal Ethical Committee of Hubei University. 40 rats were randomly divided into four groups: sham-operated rats, sham rats treated with Icariin, AngII-administrated rats, and AngII rats treated with Icariin. The hypertension model was generated by subcutaneous infusion with AngII (120 ng/min) using an implanted osmotic minipump (ALZET model 2004; Durect Corp, CA, USA) for 4 weeks. Sham-operated rats underwent the same procedure with the placement of osmotic minipumps containing 0.9% saline. After the placement of osmotic minipumps, rats were treated with Icariin (10 mg/kg/day, per day) by gavage for 4 weeks.

### Reactivity experiments

Rats were anesthetized, and basilar arteries were dissected and mounted as a ring in warm Krebs buffer (137 mmol/L NaCl, 5.4 mmol/L KCl, 2.0 mmol/L $CaCl_2$, 1.1 mmol/L $MgCl_2$, 0.4 mmol/L $NaH_2PO_4$, 5.6 mmol/L glucose, 11.9 mmol/L $NaHCO_3$) gassed with 95% $O_2$ and 5% $CO_2$ at 37 °C continuously. All artery rings were allowed a 1-h equilibration period to reach a stable resting diameter. After preparation, contractile responses were induced by increasing concentrations of AngII or Phe ($10^{-9}$–$10^{-5}$ mol/L). Concentration–response curves for AngII or Phe were conducted and expressed as a percentage of the maximal contraction induced by KCl ($5 \times 10^{-4}$ mol/L).

### Measurement of basilar artery diameter

After the isolation of basilar arteries, the tissues were mounted onto glass micropipettes filled with Krebs buffer in an organ chamber at 37 °C and allowed to equilibrate to reach a stable diameter at a distending pressure of 60 mmHg. The simultaneous changes in basilar arteries were recorded by Pressure Myograph Systems (110P, DMT, MI, USA) followed by stimulation with increasing concentrations of AngII or Phe ($10^{-9}$–$10^{-5}$ mol/L).

### Histological analyses

At the end of experimental period, rat basilar arteries were carefully isolated, embedded in optimal cutting temperature compound (Tissue-Tek, Sakura, Japan) and cut into 4-μm sections. The sections were incubated with 3% hydrogen peroxide aqueous solution and 10% goat serum to block endogenous peroxidase activity and non-specific staining, respectively. Afterwards, the sections were stained with hematoxylin and eosin for histopathological examination. Images were captured using a light microscope (BX51WI, Olympus, Tokyo, Japan). The medial cross-sectional area (CSA) was measured and calculated by ImageJ software (NIH, Maryland, USA). For α-SMA immunofluorescence staining, the sections were incubated with α-SMA antibody diluted in goat serum overnight at 4 °C. After washing with PBS 3 times, the sections were incubated with rabbit anti-mouse-cy3 secondary antibody for 1 h at room temperature. Fluorescent images were acquired using a fluorescence microscope (Zeiss Axioplan2, Zeiss, Munich, Germany).

### Cell culture

Primary human brain SMCs (HBVSMCs) were obtained from Creative Bioarray (NY, USA) and cultured in smooth muscle cell medium containing 100 U/mL penicillin, 100 μg/mL streptomycin and 10% FBS in a humidified incubator with 5% $CO_2$ and 95% $O_2$ at 37 °C.

### ROS detection

ROS level in HBVSMCs was visualized by $H_2$DCF-DA, DHE and MitoSOX Red staining. The cells were incubated with $H_2$DCF-DA (10 μmol/L), DHE (10 μmol/L) or MitoSOX Red (5 μmol/L) for 30 min at 37 °C. The images were acquired with Zeiss Axioplan2 fluorescence microscope. The fluorescence intensity was measured by ImageJ software.

### NADPH oxidase activity measurement

HBVSMCs were lysed in NADPH lysis buffer (1.0 mol/L $K_2HPO_4$, 0.1 mol/L EGTA, 0.15 mol/L phosphate and protease inhibitor cocktail, pH 7.0). After centrifugation at 12,000×*g* for 5 min, the supernatant was collected and incubated with lucigenin (5 mmol/L) for 10 min at 37 °C in the dark. The basal relative light units (RLU) of chemiluminescence were recorded using a luminometer (Promega, WI, USA). Afterwards, NADPH (100 μmol/L) was immediately added to the suspension and the chemiluminescence was recorded every 15 s for 20 min as experimental RLU. The NADPH oxidase activity was calculated as mean RLU, which were normalized to total protein concentration.

### Western blotting analysis

Human brain vascular SMCs were lysed using with RIPA buffer containing 1% protease and phosphatase inhibitors (Merck, Darmstadt, Germany). The protein concentrations of each sample were quantified using a bicinchoninic acid kit (BioRad, CA, USA). Equal amounts of protein were separated by 8–10% SDS–PAGE gels and then transferred onto polyvinylidene fluoride (PVDF) membranes (Millipore, MA, USA). After blocking by 5% non-fat milk powder in TBST (10 mmol/L Tris–HCl, 150 mmol/L NaCl, 0.05% Tween-20, pH 7.6) for 1 h, the membranes were incubated with appropriate primary antibodies at 4 °C overnight followed by incubation with HRP-conjugated secondary antibodies. The signals were visualized by enhanced chemiluminescence (Amersham Pharmacia, NJ, USA). Image quantification was performed using ImageJ software.

### Proliferation assay

Human brain vascular SMCs proliferation was determined by cell counting and BrdU assay. The cells were seeded at a density of $2 \times 10^3$ cells per well in 96-well plates. After treatments, the cells were incubated with CCK-8 reagent (Dojindo Molecular Technologies, MD, Japan) for 2 h at 37 °C. BrdU assay was performed by adding BrdU reagent to each well for 24 h of incubation to label the cells. The absorbance was determined at a wavelength of 450 nm with a microplate reader (Multiskan Spectrum, Thermo Fisher Scientific Inc., PA, USA).

### Wound healing assay

The cells were cultured to 95% confluence in 6-well plates and treated with AngII and Icariin. Afterwards, cell monolayers were scraped with a sterile 100 μL pipette tip to form wound gaps. 48 h later, the images of wound area were obtained by a light microscope.

### Invasion assay

The ability of cell invasion was examined using Transwell chambers (Costar, MA, USA) with 8-μm-pore-size polycarbonate membrane. HBVSMCs ($1 \times 10^5$ cells) were cultured in 100 μL medium with 0.5% FBS in the upper chamber and then treated with AngII and Icariin. To induce cell invasion, 10% FBS was added to the medium in the lower chamber. 48 h later, the cells in the lower chamber were fixed by 4% paraformaldehyde and stained with crystal violet. The images were captured by a light microscope.

### Quantitative PCR analysis

Total RNA from HBVSMCs was isolated using an easyBLUE total RNA extraction kit (iNtRON Biotechnology, Seoul, Korea) according to the manufacturer's instructions. The quantity of total RNA was obtained by UV spectrometry. 2 μg of RNA was reverse-transcribed to cDNA (cDNA synthesis kit, Thermo Fisher Scientific Inc.) and then subjected to real-time PCR. The reaction was performed by using LightCycler FastStart DNA SYBR Green I mix (Roche, Berlin, Germany) with an ABI 7500 RT-PCR System (Applied Biosystems, CA, USA). The primers used for PCR were as follows: Nox2 (100 bp) sense, 5′-TGTCAAGTGCCCAAAGGTGT-3′ and antisense, 5′-CCCAACGATGCGGATATGGA-3′; and GAPDH (117 bp) sense, 5′-GAAGACGGGCGGAGAGAAAC-3′ and antisense, 5′-CCATGGTGTCTGAGCGATGT-3′. The

mRNA level of each sample was normalized to the mRNA level of GAPDH.

### Statistical analysis

Data were presented as mean value ± standard error of mean (SEM). The number of samples in each experiment was indicated in figure legends. The differences between groups were analyzed by two-tailed Student *t* test or one-way ANOVA, followed by the Bonferroni multiple comparison test. Statistical analysis was performed by SPSS 18.0 software (SPSS Inc., IL, USA). $P<0.05$ was considered statistically significant.

## Results

### Icariin inhibited contractile responses in basilar arteries of AngII hypertensive rats

In basilar arteries from sham-operated rats, AngII or Phe induced contraction by a dose-dependent manner. The concentration–response curves were similar before and after Icariin treatment. However, the contractile responses to AngII or Phe were significantly potentiated in AngII hypertensive rats, but not in Icariin-treated AngII hypertensive rats (Fig. 1a, b). Expectedly, AngII or Phe induced reduction in diameter of basilar arteries, which was much pronounced in AngII hypertensive rats. Icariin treatment abolished the enhanced effects of AngII or Phe in hypertensive rats (Fig. 1c, d).

### Icariin limited cerebrovascular remodeling in hypertensive rats

We next investigated whether the inhibition of contractile responses was associated with an attenuation of cerebrovascular remodeling. Hematoxylin and eosin staining of basilar arteries revealed that the medial CSA, a typical feature of hypertrophic remodeling, was indistinguishable in sham rats before and after Icariin treatment. AngII infusion significantly increased media thickness and reduced internal lumen diameter, resulting to enhanced CSA. However, the increase of CSA was almost completely eliminated by Icariin treatment (Fig. 2a, b). Moreover, α-SMA immunofluorescence staining also showed that Icariin markedly restrained the increase of thickness of smooth muscle layer (Fig. 2c, d).

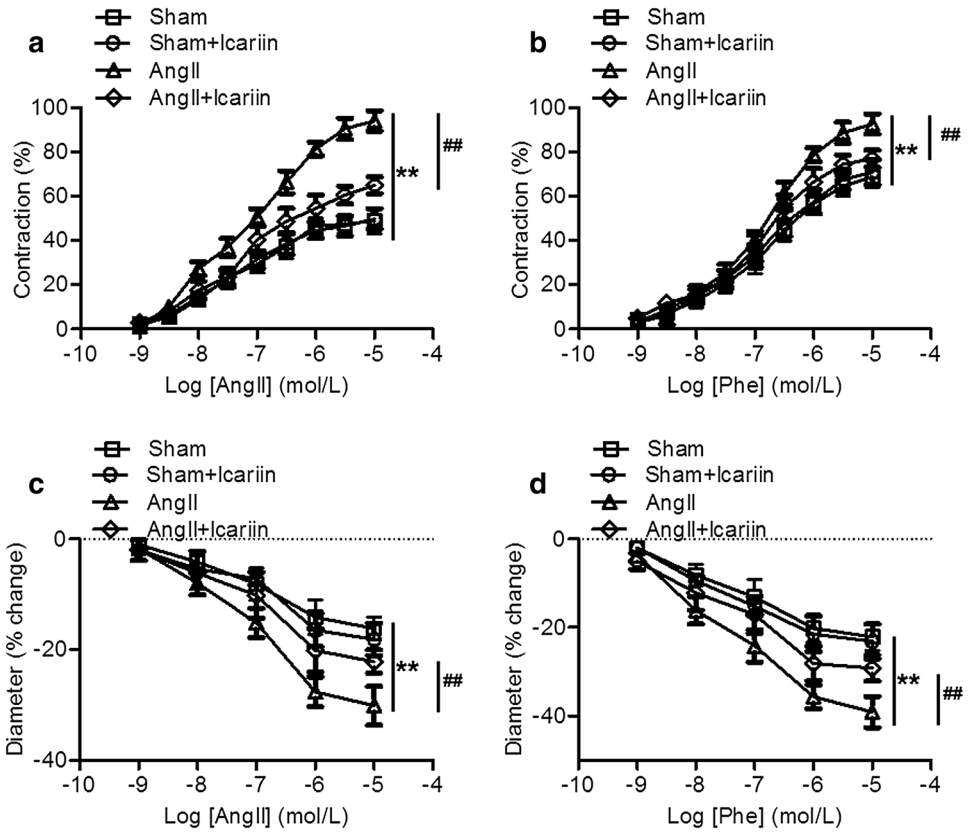


**Fig. 1** Icariin attenuates basilar artery constriction in AngII hypertensive rats. Constriction of basilar artery in response to Angiotensin II (AngII) (**a**) or phenylephrine (Phe) (**b**) in sham-operated and AngII-infused rats with or without Icariin treatment. The curves indicated that Icariin ameliorated the reduction of basilar artery diameter in response to AngII (**c**) and Phe (**d**) in AngII hypertensive rats. $^{**}P<0.01$ vs. sham; $^{\#\#}P<0.01$ vs. AngII, $n=6$

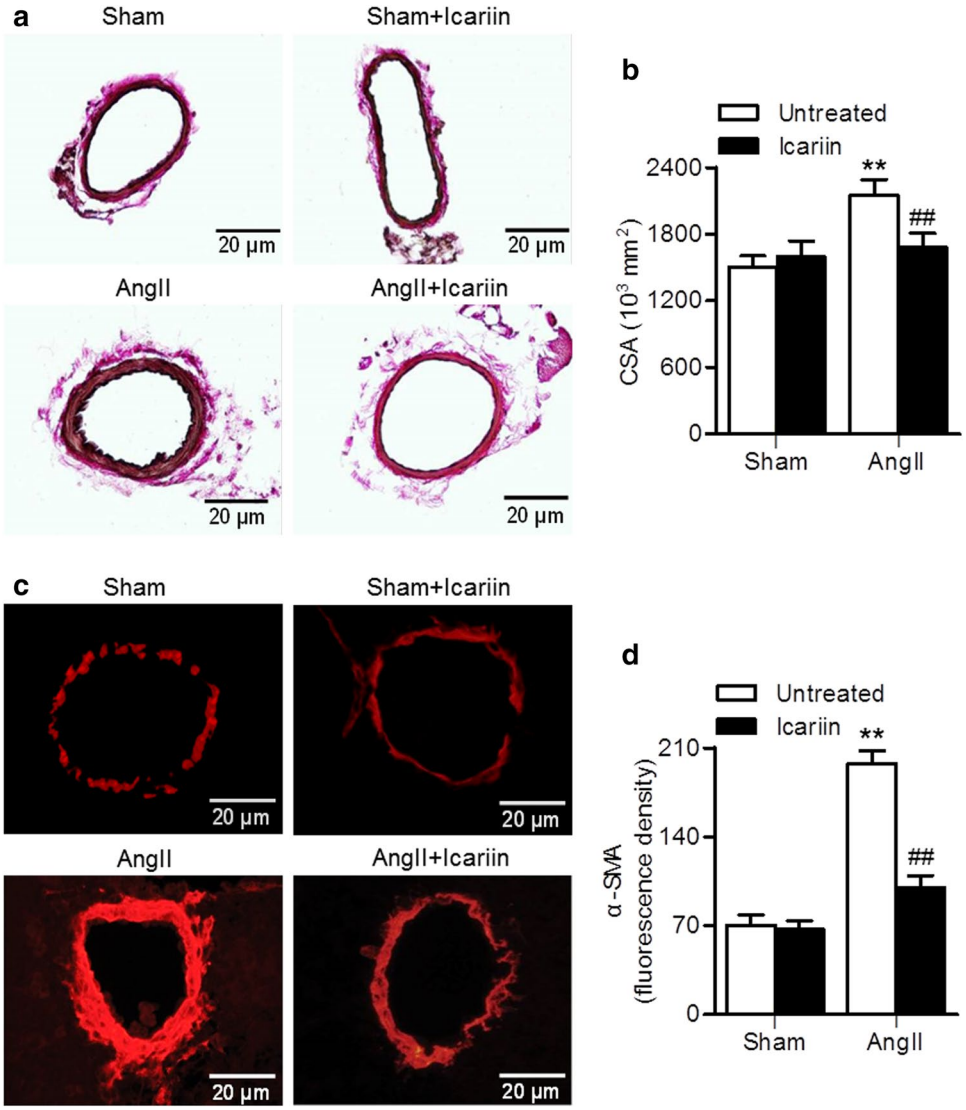


**Fig. 2** Icariin blocks cerebrovascular remodeling in AngII hypertensive rats. **a** Representative images of hematoxylin and eosin staining of basilar arteries. **b** Vascular remodeling was evaluated by cross-sectional area (CSA). **c** Representative images of immunofluorescence staining for α-SMA expression. **d** Bar graph indicates the relative fluorescence density values for α-SMA expression. $^{**}P<0.01$ vs. sham; $^{\#\#}P<0.01$ vs. AngII, $n=6$

## Icariin prevented AngII-induced HBVSMCs proliferation, migration and invasion

Cerebrovascular SMCs hyperplasia is a major contributor for cerebrovascular remodeling [2, 5]. Thus, we initially investigated the effects of Icariin on HBVSMCs proliferation. CCK-8 result showed that AngII-induced increase of cell viability was significantly inhibited after Icariin treatment (Fig. 3a). Similarly, BrdU incorporation also supported that Icariin attenuated AngII-induced proliferation of HBVSMCs (Fig. 3b). Moreover, the Transwell invasion assay showed that Icariin inhibited the invasion of HBVSMCs induced by AngII (Fig. 3c). In addition, AngII induced the migration of HBVSMCs to close the wound, while Icariin remarkably decreased the migrating distance (Fig. 3d).

## Icariin decreased AngII-induced ROS production in HBVSMCs

It has been well documented that oxidative stress is one of the major underlying mechanisms of VSMC hyperplasia [10, 12]. Intriguingly, AngII-induced proliferation of HBVSMCs was markedly attenuated by antioxidant NAC (Figure S1), indicating the involvement of oxidative stress in AngII-mediated cerebrovascular SMCs hyperplasia. To explore the possibility whether Icariin inhibits HBVSMCs proliferation via regulating the level of oxidative stress, ROS production was determined by $H_2$DCF-DA and DHE dye. Icariin treatment had no effects on ROS production under basal condition. After 48 h of AngII stimulation, the fluorescence was markedly increased, and the increase of ROS production was inhibited after Icariin treatment (Fig. 4a–d). Similarly,

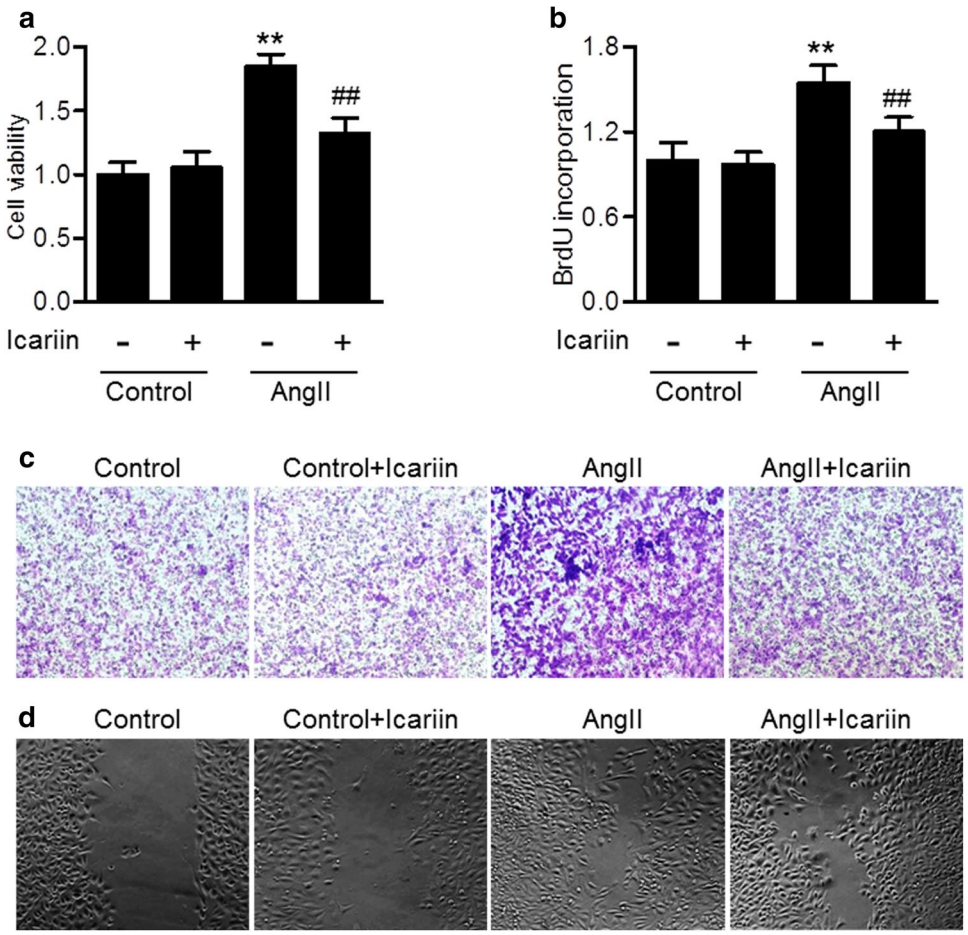


**Fig. 3** Icariin decreases AngII-induced motility of HBVSMCs. **a, b** The cells were treated with AngII ($10^{-7}$ mol/L) in the presence or absence of Icariin (20 μmol/L) for 48 h. Cell proliferation was determined by CCK-8 assay (**a**) and BrdU incorporation (**b**). $^{**}P<0.01$ vs. control; $^{\#\#}P<0.01$ vs. AngII, $n=6$. **c** HBVSMCs migration was examined by Transwell analysis. The representative images were shown. **d** Wound healing assay was performed. The representative images were shown

AngII-induced increase of ROS in basilar arteries was also attenuated in Icariin-treated rats (Figure S2A and B). We next determined how Icariin decreases AngII-induced ROS production. The results of mitochondrial ROS (mROS) production using a highly selective indicator dye MitoSOX Red showed that Icariin produced no effects on mROS production in the presence or absence of AngII stimulation (Fig. 4e, f). However, AngII significantly increased the activity of NADPH oxidase in HBVSMCs. Importantly, the increased NADPH oxidase activity was attenuated by Icariin treatment (Fig. 4g). These results suggest that Icariin abrogates the excessive ROS generation induced by AngII via inhibiting NADPH oxidase activity.

## Icariin attenuated AngII-induced NADPH oxidase activity through promoting Nox2 degradation

NADPH is an enzyme complex that composed of two membrane subunits (Nox2/gp91phox and p22phox) and four cytosolic subunits (p47phox, p67phox, p40phox and Rac1) [20]. To understand the mechanism by which Icariin decreases NADPH oxidase activity, the effect of Icariin on the above subunits expressions was determined. Although AngII increased the expression of Rac1, p47phox and p67phox in HBVSMCs, no significant changes was observed after Icariin treatment. Moreover, the expression of p22phox and p40phox remained unchanged among the groups. Interestingly, AngII-induced increase of Nox2 expression was markedly inhibited by Icariin treatment, indicating that Nox2 may be a key molecular target for Icariin in regulating NADPH oxidase activity (Fig. 5a, b). Similar results were observed in basilar arteries that Icariin also significantly decreased Nox2 expression in AngII-induced hypertensive rats (Figure S2C and D). To further investigate how Icariin decreases Nox2 expression, we next tested the mRNA level of Nox2. Although the mRNA level of Nox2 was increased after AngII stimulation, we did not detect any differences before and after Icariin treatment, suggesting a post-transcriptional regulation seems to be taking place (Fig. 5c). Moreover, the stability of Nox2 protein was examined by using a protein synthesis inhibitor CHX. Western blotting results showed that CHX treatment resulted in a time-dependent decrease of Nox2 protein expression in HBVSMCs in the presence of AngII. Icariin obviously antagonized against the degradation of Nox2, decreasing the half-life of Nox2 protein more than 5 h (Fig. 5d, e). Together, the results suggest that

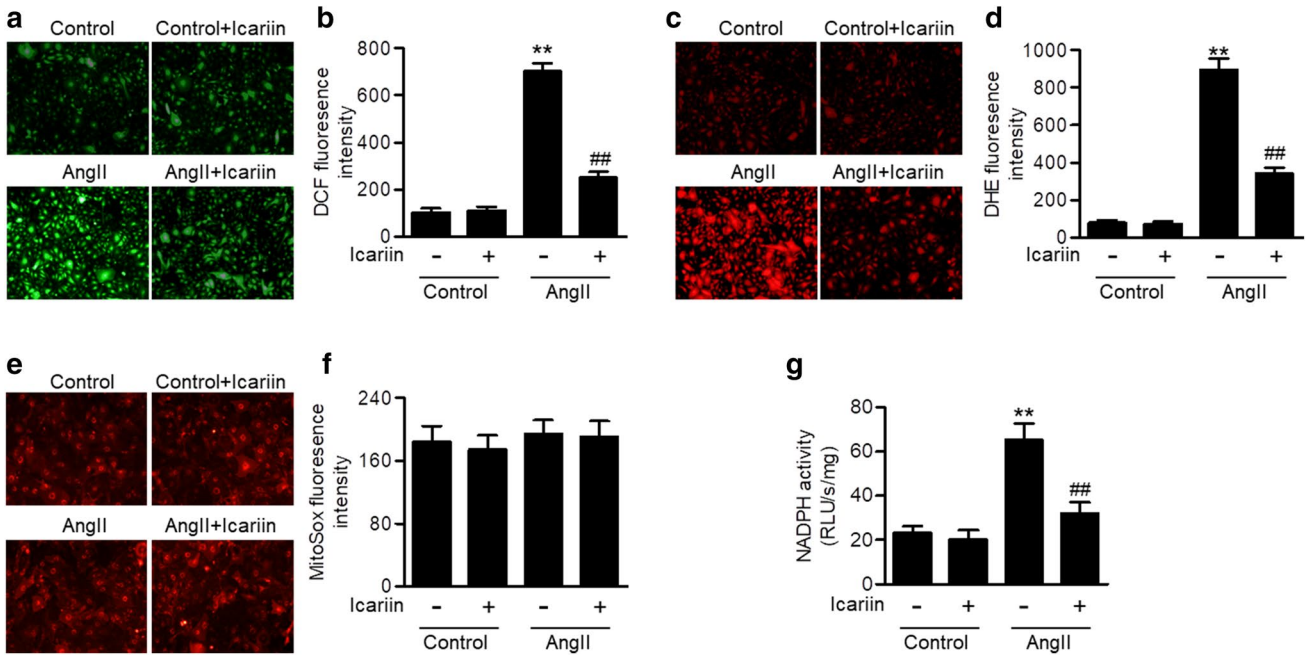


**Fig. 4** Icariin inhibits NAPDH oxidase-mediated ROS generation. **a** HBVSMCs were co-incubated with AngII ($10^{-7}$ mol/L) and Icariin (20 μmol/L) for 48 h. ROS generation was determined by $H_2$DCF-DA (10 μmol/L) staining. **b** Quantitative analysis of DCF fluorescence intensity. **c** Superoxide anion in HBVSMCs was examined by dihydroethidium (DHE) fluorescence using a fluorescence microscope. **d** Quantitative evaluation of DHE fluorescence intensity was performed. **e** Fluorescence microscope was used to localize mitochondrial ROS generation using MitoSOX Red staining. **f** Quantitative evaluation of MitoSOX fluorescence intensity. **g** Quantitation analysis of NADPH oxidase activity in HBVSMCs. $^{**}P<0.01$ vs. control; $^{\#\#}P<0.01$ vs. AngII, $n=6$

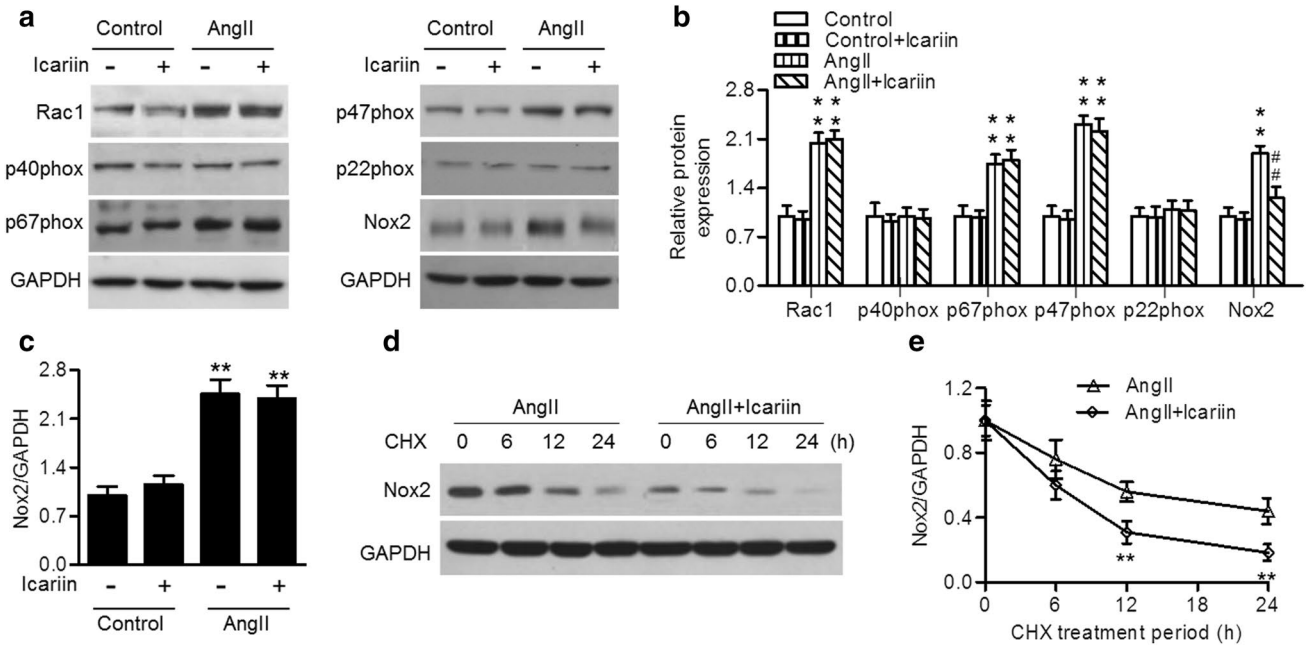


**Fig. 5** Icariin promotes Nox2 protein degradation. **a** HBVSMCs were treated with AngII ($10^{-7}$ mol/L) in the presence or absence of Icariin (20 μmol/L) for 48 h. The protein expression of Rac1, p40phox, p67phox, p47phox, p22phox and Nox2 was determined by western blotting. **b** Densitometric analysis of the above protein expression. $^{**}P<0.01$ vs. control; $^{\#\#}P<0.01$ vs. AngII, $n=6$. **c** mRNA level of Nox2 was examined by quantitative PCR. $^{**}P<0.01$ vs. control, $n=6$. **d** Western blotting analysis of Nox2 expression. After the treatment mentioned in **a**, cycloheximide (CHX) was added to the cells at 10 μg/mL for the indicated times. **e** Densitometric quantification of Nox2 level normalized to GAPDH. $^{**}P<0.01$ vs. AngII, $n=8$

Icariin reduces Nox2 expression by facilitating its protein degradation.

## Discussion

The aim of this study was to explore the protective effects of Icariin on cerebrovascular remodeling in vivo and in vitro. The results showed that Icariin significantly inhibited basilar artery contractile responses and remodeling in AngII-induced hypertensive rats. The protective effects of Icariin were related to the inhibition of Nox2-mediated NADPH activity.

Hypertension is a major risk for cerebrovascular remodeling and stroke [12]. Small arteries resistance (such as mesenteric and basilar arteries) is critical for regulating blood pressure [4]. AngII acts as a potent vasoconstrictor in SMCs for acute stimulation, and in long term, induces SMCs proliferation and vascular remodeling, which mediates physiological control of blood pressure and electrolyte balance [6, 7]. The increase of AngII level in plasma from hypertensive mice is associated with vascular remodeling [21]. Therefore, AngII-induced hypertension is suggested to be a good model for the study for vascular remodeling. Indeed, the model was also validated in this study. Our results, together with the previous studies demonstrate that AngII induces basilar artery constriction and remodeling, as well as cerebrovascular SMC proliferation, migration and invasion. These pathologic alterations were all attenuated by Icariin treatment. The data indicate that Icariin prevents cerebrovascular SMCs hyperplasia and remodeling.

Despite increasing evidence suggesting that multiple factors contribute to vascular SMCs hyperplasia, it is likely that oxidative stress functions as the major mechanism [10, 12, 22]. Excessive ROS production can activate diverse signaling, such MAPKs, HIF and NFκB, leading to SMCs proliferation [23–25]. In this study, we found that inhibition of oxidative stress with antioxidant NAC effectively reversed AngII-induced cerebrovascular SMCs proliferation. It is worth noting that Icariin could increase superoxide dismutase activity and decrease lipid peroxidation in endothelial cells, leading to blood supply and myocardial protection [26]. This finding reveals the inhibitory effects of Icariin on oxidative stress. Thus, we next examined whether Icariin influences oxidative stress level in cerebrovascular SMCs and the underlying mechanisms. Following AngII stimulation, ROS production in HBVSMCs was significantly increased, which was almost abolished by Icariin treatment. In vascular SMCs, NADPH oxidase and mitochondrial electron transport chain compose the main sources of intracellular ROS [27, 28]. Our results showed that Icariin treatment had no effects on mROS production, but dramatically inhibited AngII-induced NADPH oxidase activity. These findings suggest Icariin decreases ROS production via inhibiting NADPH oxidase activity but not mitochondria-derived ROS production.

NADPH oxidase is a complex that contains 6 subunits, Nox2, p22phox, p40phox, p47phox, p67phox and RAC1 [20]. To distinguish which subunit(s) was affected by Icariin, we determined the expression of theses subunits and showed that only Nox2 expression induced by AngII was significantly inhibited by Icariin treatment. This indicates that downregulation of Nox2 expression may underlie the inhibitory effect of Icariin on NADPH oxidase activity. Surprisingly, Icariin produced no effects on the increased Nox2 mRNA expression, suggesting transcriptional regulation is not involved. Previous studies have shown that Nox isoforms could be degraded by proteasome-dependent degradation pathway [20, 29]. Here, we evidenced that Icariin treatment decreased the half-life of Nox2 protein as compared with AngII stimulation alone, indicating Icariin promotes Nox2 degradation and subsequently decreases Nox2 protein expression.

In conclusion, this study demonstrates that Icariin treatment ameliorates cerebrovascular SMCs hyperplasia and remodeling via inhibiting Nox2-containing NADPH-derived ROS generation. Our findings may present a novel application of Icariin in the treatment of stroke.

### Compliance with ethical standards

**Conflict of interest** The authors declare that they have no conflict of interest.

## References

1. Maghbooli Z, Hossein-Nezhad A. Transcriptome and molecular endocrinology aspects of epicardial adipose tissue in cardiovascular diseases: a systematic review and meta-analysis of observational studies. BioMed Res Int. 2015;2015:926567. https://doi.org/10.1155/2015/926567.
2. Roger VL, Go AS, Lloyd-Jones DM, Adams RJ, Berry JD, Brown TM, Carnethon MR, Dai S, de Simone G, Ford ES, Fox CS, Fullerton HJ, Gillespie C, Greenlund KJ, Hailpern SM, Heit JA, Ho PM, Howard VJ, Kissela BM, Kittner SJ, Lackland DT, Lichtman JH, Lisabeth LD, Makuc DM, Marcus GM, Marelli A, Matchar DB, McDermott MM, Meigs JB, Moy CS, Mozaffarian D, Mussolino ME, Nichol G, Paynter NP, Rosamond WD, Sorlie PD, Stafford RS, Turan TN, Turner MB, Wong ND, Wylie-Rosett J, American Heart Association Statistics Committee and Stroke Statistics Subcommittee. Heart disease and stroke statistics–2011 update: a report from the American Heart Association. Circulation. 2011;123(4):e18–209. https://doi.org/10.1161/CIR.0b013e3182009701.
3. Chen R, Kang R, Fan XG, Tang D. Release and activity of histone in diseases. Cell Death Dis. 2014;5:e1370. https://doi.org/10.1038/cddis.2014.337.
4. Feihl F, Liaudet L, Waeber B, Levy BI. Hypertension: a disease of the microcirculation? Hypertension. 2006;48(6):1012–7. https://doi.org/10.1161/01.HYP.0000249510.20326.72.

5. Feihl F, Liaudet L, Waeber B. The macrocirculation and microcirculation of hypertension. Curr Hypertens Rep. 2009;11(3):182–9.
6. Yaghini FA, Song CY, Lavrentyev EN, Ghafoor HU, Fang XR, Estes AM, Campbell WB, Malik KU. Angiotensin II-induced vascular smooth muscle cell migration and growth are mediated by cytochrome P450 1B1-dependent superoxide generation. Hypertension. 2010;55(6):1461–7. https://doi.org/10.1161/HYPERTENSIONAHA.110.150029.
7. Ohtsu H, Suzuki H, Nakashima H, Dhobale S, Frank GD, Motley ED, Eguchi S. Angiotensin II signal transduction through small GTP-binding proteins: mechanism and significance in vascular smooth muscle cells. Hypertension. 2006;48(4):534–40. https://doi.org/10.1161/01.HYP.0000237975.90870.eb.
8. Chan SH, Chan JY. Angiotensin-generated reactive oxygen species in brain and pathogenesis of cardiovascular diseases. Antioxid Redox Signal. 2013;19(10):1074–84. https://doi.org/10.1089/ars.2012.4585.
9. Wang XM, Xiao H, Liu LL, Cheng D, Li XJ, Si LY. FGF21 represses cerebrovascular aging via improving mitochondrial biogenesis and inhibiting p53 signaling pathway in an AMPK-dependent manner. Exp Cell Res. 2016;346(2):147–56. https://doi.org/10.1016/j.yexcr.2016.06.020.
10. Barman SA, Fulton D. Adventitial fibroblast Nox4 expression and ROS signaling in pulmonary arterial hypertension. Adv Exp Med Biol. 2017;967:1–11. https://doi.org/10.1007/978-3-319-63245-2_1.
11. Jeong EM, Liu M, Sturdy M, Gao G, Varghese ST, Sovari AA, Dudley SC Jr. Metabolic stress, reactive oxygen species, and arrhythmia. J Mol Cell Cardiol. 2012;52(2):454–63. https://doi.org/10.1016/j.yjmcc.2011.09.018.
12. Pires PW, Deutsch C, McClain JL, Rogers CT, Dorrance AM. Tempol, a superoxide dismutase mimetic, prevents cerebral vessel remodeling in hypertensive rats. Microvasc Res. 2010;80(3):445–52. https://doi.org/10.1016/j.mvr.2010.06.004.
13. Li C, Li Q, Mei Q, Lu T. Pharmacological effects and pharmacokinetic properties of icariin, the major bioactive component in Herba Epimedii. Life Sci. 2015;126:57–68. https://doi.org/10.1016/j.lfs.2015.01.006.
14. Lan TH, Chen XL, Wu YS, Qiu HL, Li JZ, Ruan XM, Xu DP, Lin DQ. 3,7-Bis(2-hydroxyethyl)icaritin, a potent inhibitor of phosphodiesterase-5, prevents monocrotaline-induced pulmonary arterial hypertension via NO/cGMP activation in rats. Eur J Pharmacol. 2018;829:102–11. https://doi.org/10.1016/j.ejphar.2018.04.011.
15. Shi Y, Yan W, Lin Q, Wang W. Icariin influences cardiac remodeling following myocardial infarction by regulating the CD147/MMP-9 pathway. J Int Med Res. 2018;46(6):2371–85. https://doi.org/10.1177/0300060518762060.
16. Song YH, Cai H, Gu N, Qian CF, Cao SP, Zhao ZM. Icariin attenuates cardiac remodelling through down-regulating myocardial apoptosis and matrix metalloproteinase activity in rats with congestive heart failure. J Pharm Pharmacol. 2011;63(4):541–9. https://doi.org/10.1111/j.2042-7158.2010.01241.x.
17. Hu YW, Liu K, Yan MT. Effect and mechanism of icariin on myocardial ischemia-reperfusion injury model in diabetes rats. Zhongguo Zhong Yao Za Zhi. 2015;40(21):4234–9.
18. Qian ZQ, Wang YW, Li YL, Li YQ, Ling Z, Yang DL. Icariin prevents hypertension-induced cardiomyocyte apoptosis through the mitochondrial apoptotic pathway. Biomed Pharmacother. 2017;88:823–31. https://doi.org/10.1016/j.biopha.2017.01.147.
19. Hu YW, Li HT, Liu K, Yan MT, Zhang Y, Ren LQ. Effects of icariin on proliferation of vascular smooth muscle cell induced by ox-LDL via impacting MAPK signaling pathway. Zhongguo Zhong Yao Za Zhi. 2016;41(19):3655–60. https://doi.org/10.4268/cjcmm20161926.
20. Noubade R, Wong K, Ota N, Rutz S, Eidenschenk C, Valdez PA, Ding J, Peng I, Sebrell A, Caplazi P, DeVoss J, Soriano RH, Sai T, Lu R, Modrusan Z, Hackney J, Ouyang W. NRROS negatively regulates reactive oxygen species during host defence and autoimmunity. Nature. 2014;509(7499):235–9. https://doi.org/10.1038/nature13152.
21. Wang M, Yang H, Zheng LY, Zhang Z, Tang YB, Wang GL, Du YH, Lv XF, Liu J, Zhou JG, Guan YY. Downregulation of TMEM16A calcium-activated chloride channel contributes to cerebrovascular remodeling during hypertension by promoting basilar smooth muscle cell proliferation. Circulation. 2012;125(5):697–707. https://doi.org/10.1161/CIRCULATIONAHA.111.041806.
22. Wilkinson-Berka JL, Rana I, Armani R, Agrotis A. Reactive oxygen species, Nox and angiotensin II in angiogenesis: implications for retinopathy. Clin Sci. 2013;124(10):597–615. https://doi.org/10.1042/CS20120212.
23. Ma Y, Zhang JX, Liu YN, Ge A, Gu H, Zha WJ, Zeng XN, Huang M. Caffeic acid phenethyl ester alleviates asthma by regulating the airway microenvironment via the ROS-responsive MAPK/Akt pathway. Free Radic Biol Med. 2016;101:163–75. https://doi.org/10.1016/j.freeradbiomed.2016.09.012.
24. Lu QB, Wan MY, Wang PY, Zhang CX, Xu DY, Liao X, Sun HJ. Chicoric acid prevents PDGF-BB-induced VSMC dedifferentiation, proliferation and migration by suppressing ROS/NFkappaB/mTOR/P70S6K signaling cascade. Redox Biol. 2018;14:656–68. https://doi.org/10.1016/j.redox.2017.11.012.
25. Hu H, Ding Y, Wang Y, Geng S, Liu J, He J, Lu Y, Li X, Yuan M, Zhu S, Zhao S. MitoKATP channels promote the proliferation of hypoxic human pulmonary artery smooth muscle cells via the ROS/HIF/miR-210/ISCU signaling pathway. Exp Ther Med. 2017;14(6):6105–12. https://doi.org/10.3892/etm.2017.5322.
26. Xiang J, Zhao J, Wang Y, Hua X, Huang H, Lei Y. Effect of icariin on hypoxia/reoxygenation injury in neonatal rat cardiomyocytes. Zhonghua yi xue za zhi. 2015;95(45):3701–4.
27. Forstermann U. Oxidative stress in vascular disease: causes, defense mechanisms and potential therapies. Nat Clin Pract Cardiovasc Med. 2008;5(6):338–49. https://doi.org/10.1038/ncpcardio1211.
28. Bedard K, Lardy B, Krause KH. NOX family NADPH oxidases: not just in mammals. Biochimie. 2007;89(9):1107–12. https://doi.org/10.1016/j.biochi.2007.01.012.
29. Zhao Q, Zhang J, Wang H. PGC-1alpha limits angiotensin II-induced rat vascular smooth muscle cells proliferation via attenuating NOX1-mediated generation of reactive oxygen species. Biosci Rep. 2015;35(5):e00252. https://doi.org/10.1042/BSR20150112.